Analysis and experimental validation of the figure of merit for piezoelectric energy harvesters

Daniella B. Deutz[1,2], John-Alan Pascoe[1,3], Ben Schelen[4], Sybrand van der Zwaag[1], Dago M. de Leeuw[1] and Pim Groen[1,5]*

[1] Faculty of Aerospace Engineering, Delft University of Technology, Delft, The Netherlands

[2] University Library, University of Southern Denmark, Odense, Denmark

[3] Department of Aeronautics, Imperial College London, London, United Kingdom

[4] DEMO, Corporate Services, EWI, Delft University of Technology, Delft, The Netherlands

[5] Holst Centre, Eindhoven, The Netherlands

*E-mail: dbd@bib.sdu.dk

Abstract

Piezoelectric energy harvesters are at the front of scientific research as enabler of renewable, sustainable energy for autonomous wireless sensor networks. Crucial for this disruptive technology is the achievable output power. Here we show, analytically, that the maximum output energy per unit volume, under a single sinusoidal excitation, is equal to $1/(4-2k^2)*1/2dgX^2$, where k^2 is the electromechanical coupling coefficient, d and g are the piezoelectric charge and voltage coefficient, respectively, and X is the applied stress. The expression derived is validated by the experimentally measured output energy for a variety of piezoelectric materials over an unprecedented range of more than five orders of magnitude. As the prefactor $1/(4-2k^2)$ varies only between ½ and ¼ the figure of merit for piezoelectric materials for energy harvesters is not k^2, as commonly accepted for vibrational harvesters, but dg. The figure of merit does not depend on the compliance, or Young's modulus. Hence we argue that commonly used brittle inorganic piezoelectric ceramics can be replaced by soft, mechanically flexible polymers and composite films, comprising inorganic piezoelectric materials embedded in a polymer matrix.

1. Introduction

The ability to deliver sustainable power to a wireless sensor network is attractive as it eliminates the time and cost of replacing batteries. This holds especially for networks that are either inhospitable or difficult to reach, such as structure-embedded microsystems and medical implants. The most attractive energy source is that of ambient mechanical vibrations, such as human motion, kitchen appliances and car engines. There are various methods to harvest the mechanical energy but, for small electronic harvesters, the most widely investigated effect is piezoelectricity.[1-8] The direct effect is used, where application of a mechanical stress generates an output voltage. Below a volume of about 1 cm^3, the power density for piezoelectric transduction exceeds that for electromagnetic and electrostatic generators.[9-11] Estimations for the generated power range from 0.5 to 100 mW/cm^3 for vibrations with acceleration of $1 - 10$ m/s^2 at a frequency of $50 - 350$ Hz.[12, 13] This means that with the ongoing decreasing power consumption of integrated circuits, autonomous microsystems come within reach.[14]

As discussed in many review papers,[9-12, 14-19] piezoelectric energy harvesting comprises three major steps, *viz.* mechanical-mechanical energy conversion, mechanical-electrical energy transduction and electrical energy-electrical energy output transfer. The mechanical transformer converts the inertial or kinematic energy of the source into non-translational energy in the piezoelectric material. Challenges are impedance matching and preventing mechanical failure under large stresses. Numerous mechanical designs are being used to optimize the strain, such as bimorph cantilevers, unimorph diaphragms and cymbal transducers.[20-25] The maximum amount of energy is stored at resonance. The stored energy decreases rapidly away from the resonant frequency. Not surprisingly therefore, strategies are being pursued to increase the bandwidth of the harvester, such as tunable resonators and multi-frequency arrays.[26-28]

The transduction between mechanical and electrical energy in the piezoelectric material is governed by the electromechanical coupling coefficient, k^2, which is the ratio between stored mechanical energy and input electrical energy, or *vice versa*. The value of k^2 is between 0 and 1. Most widely used are lead zirconium titanate ceramics (PZT) with k^2 of about 0.5.[29, 30]

The dynamically stimulated piezoelectric generators produce an AC current while a DC current output is needed to power electronics. To that end the AC current is rectified by diodes and stored in a capacitor or rechargeable battery.[31] Switches and inductors are used for current regulation as well as for current limiting and short-time energy storage, respectively.[13, 32, 33] The efficiency is about 50%, limited by *e.g.* power consumption and mismatch between electrical output impedance of transducer and input impedance of the electrical circuit.

Research is focused on maximizing the strain in the mechanical conversion[20-25] and on maximizing the electromechanical coupling coefficient, k^2, of the piezoelectric transducer.[34] Optimization of k^2 is not surprising as it represents the ratio between stored electrical energy and input mechanical energy. Therefore, most piezoelectric harvesters are based on PZT ceramics. However, counter intuitively, energy harvesters have been reported that use piezoelectric materials with orders of magnitude lower values of k^2, *viz.* polyvinylidefluoride (PVDF) with $k^2 \sim 0.03$[35-38], ferroelectrets with $k^2 \sim 0.005$[39-41], and low modulus piezoelectric nanogenerators based on ZnO and $BaTiO_3$.[42-44] To solve this apparent discrepancy we analyzed the performance of a piezoelectric energy harvester. We will show that the figure of merit for the output energy is not k^2, but dg where d is the piezoelectric charge coefficient and g is the piezoelectric voltage coefficient.

To verify the figure of merit,[45-51] we needed to measure the output of a harvester based on a variety of piezoelectric materials. We note, however, that the output energy strongly depends on the boundary conditions of the applied mechanical load. To circumvent the mechanical constraints, we therefore measured the output energy in the simple boundary condition of a clamped disk. This is, experimentally, the only way to reliably compare a variety of piezoelectric materials under identical conditions.

Unfortunately, due to the clamping, the output energy reduces to only nJ/cm^3. To overcome this limitation, we built an extremely sensitive piezometer system, which measures the output energy of a clamped disk under a well-defined sinusoidal mechanical excitation. We measured a variety of material classes with widely varying piezoelectric and mechanical constants. For the first time, we could experimentally validate over many orders of magnitude that the figure of merit is not k^2, but dg. This has dramatic consequences for optimization of piezoelectric materials for energy harvesting. The figure of merit does not depend on the compliance. Hence, we have an additional degree of freedom to optimize the energy harvester.

Instead of brittle ceramics, soft and mechanically flexible polymers and composite films, comprising inorganic piezoelectric materials embedded in a polymer matrix, can be applied.

This paper is organized as follows. First, an analytical expression for the output energy of a piezoelectric harvester is derived. The figure of merit and the efficiency are discussed. Next, the piezometer system, developed to measure the output energy under sinusoidal excitation with high sensitivity, is presented. Then, we will present values for the stored electrical energy measured at open circuit. Measurements were performed on intermediate polarization states of a PZT ceramic. Apart from ceramics, we also measured a wide variety of piezoelectric material classes ranging from the polymer β-PVDF, through 1-3 oriented PZT fibers embedded in epoxy, to mechanically flexible films of 0-3 random and quasi 1-3 oriented composites of both PZT and lead free KNLN particles in epoxy, PDMS and Zn ionomer matrices. Subsequently, the output energy is extracted using a resistive load. We will show that the experimentally measured output energy and open circuit stored energy as a function of piezoelectric constants and applied force can quantitatively be described, validating the analytically derived expressions.

2. Figure of Merit of a Piezoelectric Energy Harvester

2.1. *Electromechanical coupling coefficient, k^2.*

The electrical displacement, D, of a piezoelectric capacitor under applied electric field, E, is the sum of the induced, P_i, and spontaneous polarization P_s:

$$D = P_i + P_s = \varepsilon_r \varepsilon_0 E + P_s \tag{1}$$

where ε_0 is the vacuum permittivity and ε_r is the relative dielectric constant. In the following we assume that the change in spontaneous polarization with electric field can be disregarded. Basically this means that the applied electric field is much smaller than the coercive field. The electrical energy stored in the capacitor per unit volume is then given by:

$$U_{elect} = \frac{1}{2} DE = \frac{1}{2} \varepsilon_r \varepsilon_0 E^2 \tag{2}$$

Application of the electric field induces a strain, x:

$$x = dE \tag{3}$$

where d is the piezoelectric charge coefficient. We note that the charge coefficient is a fourth rank tensor, commonly written with two indices following Voigt's notation, here for clarity ignored, as we only consider compressive stress in the poling direction, parallel to the surface normal. As there is no external stress, the mechanical energy stored per unit volume is given by:

$$U_{mech} = \frac{1}{2}x^2/s = \frac{1}{2}(dE)^2/s \tag{4}$$

where s is the compliance. The electromechanical coupling coefficient, k^2, which is defined as:

$$k^2 = \frac{stored\ mechanica\ energy}{input\ electrical\ energy} = \frac{stored\ electrical\ energy}{input\ mechanica\ energy} \tag{5}$$

is then given by:

$$k^2 = d^2/\varepsilon_0 \varepsilon_r \, s = dg/s = dgY \tag{6}$$

where Y is the Young's modulus, g is the piezoelectric voltage coefficient, given by $d/\varepsilon_o \varepsilon_r$, and $0 \leq k^2 \leq 1$. We note that the stored electrical and mechanical energy are both internal energies. We will measure the electrical energy as outside work. Only when we calculate the outside work do we make a distinction between electrical and mechanical energy.

2.2. *Transmission coefficient and internal efficiency of a piezoelectric harvester*

The piezoelectric capacitor acts as a transducer as it can convert mechanical energy into electrical energy and *vice versa*. The transmission coefficient, λ, is the ratio of output energy over input energy.[52-54] For a linear transducer:

$$\lambda = \frac{output\ mechanical\ energy}{input\ electrical\ energy}, \text{ or equivalently } \lambda = \frac{output\ electrical\ energy}{input\ mechanical\ energy} \tag{7}$$

5

We calculate the transmission coefficient for the maximum mechanical work done by a piezoelectric transducer upon application of an electric field. To use a piezoelectric capacitor as a mechanical transducer we need a mechanical load. With zero mechanical load, or complete clamped conditions (*i.e.* no strain), no energy is sent to the outside world. We take the simplest case where a mass is put on the piezoelectric capacitor. The mechanical load yields a constant compressive stress, *X, i.e.* $X < 0$. The stress of the load induces a strain, *x*, of *sX* and an electrical displacement of *dX*. Although the convention is to use *T* for strain and *S* for stress, here we use *x* and *X*, respectively, to prevent confusion with other symbols, such as compliance, *s*. The load generates a mechanical input energy of ½ *xX*, which is ½ *sX²*. In open circuit the total displacement is zero. An electric field is built up:

$$E = -d/\varepsilon_0\epsilon_r X \ = \text{-}gX \tag{8}$$

leading to a stored electrical energy of:

$$U_{open} = \frac{1}{2}\varepsilon_0\epsilon_r E^2 = \frac{1}{2}\varepsilon_0\epsilon_r(-gX)^2 = \frac{1}{2}dgX^2 \tag{9}$$

Next, the electrodes are grounded to annihilate the excess charges. Then, in order to generate an outside stress, an electric field, *E,* is applied. This field yields an additional strain of *dE*. The total strain is then given by:

$$x = sX + \ dE \tag{10}$$

and the mechanical output energy is given by:

$$U_{out} = \frac{1}{2}xX = \ \frac{1}{2}(sX + dE)X \tag{11}$$

Without external load, the stress, *X*, and the output energy are both zero. For a given compressive load, $X < 0$, the output energy depends on the value of the electric field. For small values, the strain due to the electric field is smaller than the strain induced by the load. The output energy then is positive, meaning that all energy remains stored in the transducer; no outside work is done. With increasing electric field, the strain due to the electric fields gets equal to the strain induced by the load; then the total strain and output energy are both zero.

At higher values of the electric field the total strain and output energy gets negative and work is done to the outside world. For a given electric field, the maximum outside work is obtained when the derivative dU_{out}/dX is zero:

$$U_{out,max} = -\frac{1}{8}(dE)^2/s = -\frac{1}{2}sX^2 \text{ when } X = -dE/2s \tag{12}$$

This means that the maximum output energy is obtained when the strain induced by the external load is half of the strain generated by the electric field, *i.e. X/E* is equal to *-d/2s*. Furthermore, the maximum output energy is exactly equal to the stored mechanical energy of the applied compressive load, *viz. ½sX²*.

The corresponding input electrical energy follows from the displacement as:

$$U_{elect,in} = \frac{1}{2}DE = \frac{1}{2}(\varepsilon_r\varepsilon_0 E + dX)E = \frac{1}{2}\left(\varepsilon_r\varepsilon_0 E + d\left(-\frac{dE}{2s}\right)\right)E \tag{13}$$

and the transmission coefficient, λ, for this maximum output energy is then:

$$\lambda_{max\,output} = \frac{1}{8}((dE)^2/s)/((\frac{1}{2}\left(\varepsilon_r\varepsilon_0 E + d\left(-\frac{dE}{2s}\right)\right)E)$$

$$= \frac{1}{4}(d^2/s)/(\varepsilon_r\varepsilon_0 - \frac{d^2}{2s}) = k^2/(4-2k^2) \tag{14}$$

where we have used $k^2 = dg/s$, *c.f.* eqn. (6). The limiting values for $\lambda_{max\,output}$ are $\frac{1}{4}k^2$ for small values of k^2 and $\frac{1}{2}k^2$ for k^2 approaching unity.

In literature, researchers have focused on the maximum transmission coefficient instead of on the coefficient for maximum output.[52-54] As derived in the electronic supplementary information (ESI) Section 2, this maximum transmission coefficient is given by:

$$\lambda_{max} = \left(1/k + \sqrt{(1/k)^2 - 1}\right)^{-2} \cong k^2/(4-2k^2) \tag{15}$$

Only at low values of k^2 below about 0.5 the transmission coefficients are equal, *viz. k²/(4-2k²)*. At very high values of k^2, approaching 1, there is a significant difference. The transmission coefficient for maximum output energy, $\lambda_{max\,output}$, goes to $\frac{1}{2}k^2$ while the maximum transmission coefficient goes to unity. We note that the maximum transmission

coefficient is obtained when the strain induced by the external load is almost equal to the strain generated by the electric field. However, this situation is practically useless as then the total strain and, hence the output power, both go to zero. A classical problem, the maximum transmission coefficient is unity but under that constraint you cannot harvest energy. As this situation is irrelevant, it is dealt with in ESI Section 2.

The expression for the transmission coefficient is derived using the electrical input energy in the first work cycle. This energy however is not lost but remains stored as electrostatic energy in the capacitor, where it can be used in the next work cycle. Hence the internal efficiency of the transducer is almost 100%.[54] The only energy loss is the dielectric loss of the capacitor, which is typically below 3%. The transmission coefficient therefore is not a measure of efficiency; it represents the fraction of the stored mechanical energy that can externally be harvested, and *vice versa*.

We consider an energy harvester as consisting of a transducer coupled to an oscillating spring. When there is no damping to inelastic losses, all the mechanical energy remains stored in the spring. The transducer converts a fraction of the stored mechanical energy, *viz.* the transmission coefficient, into electrical energy. When the dielectric loss can be disregarded, the internal efficiency describing the conversion of absorbed, stored mechanical energy into electrical energy is unity.

2.3. *Figure of Merit (FOM)*

At first sight, it seems that the performance of the harvester is dominated by the transmission coefficient. However, not the transmission coefficient but the maximum output energy is the decisive parameter. The output energy of the harvester is given by:

$$U_{out,max} = \frac{1}{2}sX^2 * \frac{k^2}{4-2k^2} = \frac{1}{4-2k^2} * \frac{1}{2}dgX^2 = \frac{1}{4-2k^2}U_{open}. \tag{16}$$

where eqn. (9) is used for the stored electrical energy in open circuit. Firstly, this equation implies that the maximum output energy is a fraction $1/(4-2k^2)$ of the stored electrical energy in open circuit. This fraction varies between ½ and ¼ depending on k^2. Here we have assumed that all of the output energy can be electrically converted, meaning that the efficiency for the harvesting electronics is 100%, albeit that in practice a value of 50% is more realistic.

8

Secondly, the prefactor $1/(4-2k^2)$ hardly depends on the value of k^2: the output energy is about 1/8-1/4 times dgX^2. Hence the figure of merit of a piezoelectric energy harvester is dominated by dg.

The figure of merit can be understood by the following simple argument. Firstly, when stress is applied to a piezoelectric transducer, the energy is used to charge the piezoelectric capacitor. The output energy is proportional to the stored electrical energy, $\frac{1}{2} dgX^2$, which therefore only depends on the piezoelectric voltage and charge coefficient. More specifically, the electrical output energy is the transmission coefficient times the input energy. The transmission coefficient is a fraction of k^2 and the mechanical input energy $\frac{1}{2} sX^2$. As k^2 is equal to dg/s, the output energy only depends on dg as the compliance is cancelled out. In the past, researchers have focused on increasing the electromechanical coupling coefficient, k^2. Piezoelectric polymers and flexible composites with very low k^2 values due to a large compliance, or small Young's modulus, therefore were considered inappropriate. However, the stored mechanical energy, $1/2sX^2$, is therefore large and, consequently, the output energy does not depend on the compliance. Hence, we have an additional degree of freedom to optimize the piezoelectric transduction in an energy harvester. Instead of brittle ceramics, soft and mechanically flexible materials with a small compliance can be used, such as piezoelectric polymers and composite films, comprising inorganic piezoelectric materials embedded in a polymer matrix.

3. Piezometer System to Measure the Stored and Harvested Electrical Energy

We built a piezometer system to quantitatively relate the stored electrical energy with the piezoelectric charge and voltage coefficients, d and g, for any piezoelectric material. We note that the output energy strongly depends on the boundary conditions of the applied mechanical load. As discussed in detail in ESI Section 3 and 4, the mechanical input energy can easily vary over six orders of magnitude. The only way to compare the intrinsic performance of different materials is to measure a circular disk of a piezoelectric material in clamped conditions. In this geometry there is no shear or bending. However, due to this boundary condition there is limited strain, which is estimated for a clamped PZ27 disk to be only 0.003% under 10 N of dynamic force. This means that there is hardly any stored electrical energy. Therefore the piezometer system is developed to be extremely sensitive, able to detect

stored energy in the order of nJ/cm^3. The working principle of the piezometer system, force transfer, temperature control, and data extraction are discussed in detail in ESI Section 5.

A schematic representation of the piezometer system, operating under quasi-static load, is presented in Fig. 1a. A photograph of the jig is presented in Fig. 1b. The sample is placed between two rounded calibers. The sample is metallized on both sides, yielding a piezoelectric capacitor. An inductive voice coil supplies both a static and dynamic force, $F(\omega t) = F_{max} f(\omega t)$, where $f(\omega t)$ is a periodic function of time, t, and ω is the angular frequency. The force is applied to the sample through a metal rod, isolated by a Macor mount, and connected to one of the Berlincourt calibers. The polarization of the sample is in line with the direction of the force. The dynamic force generates a piezoelectric charge on the surfaces of the piezoelectric sample, $Q(\omega t) = Q_{max} f(\omega t)$.[55]

As a typical example we present measurements on a widely studied,[55, 56] commercial, soft PZT, PZ27 ceramic disk. The diameter is 10 mm and the thickness, t, is around 1 mm. The applied force is presented in Fig. 1c and shows a dynamic sinusoidal force of 1.5 N at a frequency of 1 Hz, superimposed with a static force of 10 N.

The short circuit current, I_{SC}, is presented in Fig. 1d. The current is the derivative of the force, which for the sinusoidal excitation translates to an offset of almost 90°. We note that the piezoelectric loss, $tan\ \delta_p$, can be calculated from the phase difference between applied force and output signal. The phase difference is not exactly 90°, but typically 3° to 5° off, in the range of forces examined here. The calculated loss is small, and can be disregarded.

The short circuit current is used to confirm the accuracy of the set dynamic force. The calculated piezoelectric charge coefficient, d_{33}, as calculated from I_{SC} matches the independently measured charge coefficient from the Berlincourt piezometer well.

The open circuit voltage, V_{OC}, is presented as a function of time in Fig. 1e. The voltage is the second derivative of the applied force, which for a sinusoidal excitation is equal to the original excitation waveform. It is crucial to note that the magnitude of the generated voltage is independent of the contact area, $A_{caliber}$, it only depends on the total electroded surface area of the piezoelectric capacitor, A_{sample}.

$$D = dX = d \frac{F}{A_{caliber}} \tag{17}$$

Hence,

$$Q = DA_{caliber} = dF \tag{18}$$

and the total generated charge, Q, and hence the open circuit voltage V_{OC}, are independent of the area of the caliber. We can now calculate the stored electrical energy per unit volume of the piezoelectric capacitor, U_{open}, given as:

$$U_{open} = \frac{1}{2} C V_{OC}^2 / A_{sample} t \tag{19}$$

$$= \frac{1}{2} C \left(\frac{Q}{C}\right)^2 / A_{sample} t = \frac{1}{2C} Q^2 / A_{sample} t = \frac{1}{2\varepsilon_0 \varepsilon_r} \frac{t}{A_{sample}} (dF)^2 / A_{sample} t$$

$$= \frac{1}{2} dg \left(F/A_{sample}\right)^2 \tag{20}$$

which is similar to eqn. (9). The energy per unit volume does not explicitly depend on the sample thickness. Furthermore, this energy depends on the surface area of the capacitor, but is independent of the contact area of the caliber. The reason is that the whole area of the capacitor is metallized. Furthermore, due to the clamping, there is no shear or bending and only d_{33} has to be considered. The scaling of the stored energy per unit area, U_{open}, with sample thickness and sample area will be experimentally validated in Section 5 below.

The stored electrical energy, per unit volume, is presented as a function of time in Fig. 1f, based on the V_{OC}, as shown in Fig. 1e. As U_{open} depends on V_{OC}^2, it oscillates at double the applied frequency. The energy density is relatively low, only in the range of nJ/cm^3. The first reason is that the sample is clamped. The second reason is that the sample area in this example is relatively large, a diameter of 1 cm, yielding a large volume and concomitantly a small energy density.

We note that the small stored electrical energies can be accurately determined in the developed piezometer system because the applied force is accurately applied. Furthermore, we measure V_{OC}, in the range of mV to V, rather than the typical I_{SC}, in the pA to nA range. The focus on V_{OC}, especially allows for accurate measurement of materials, such as PVDF

and composites, with low d_{33}, below 30 pC/N, but a relatively high g_{33}, up to 200 mV m/N. In summary, the developed piezometer system allows accurate measurement of the stored electrical energy for any piezoelectric material.
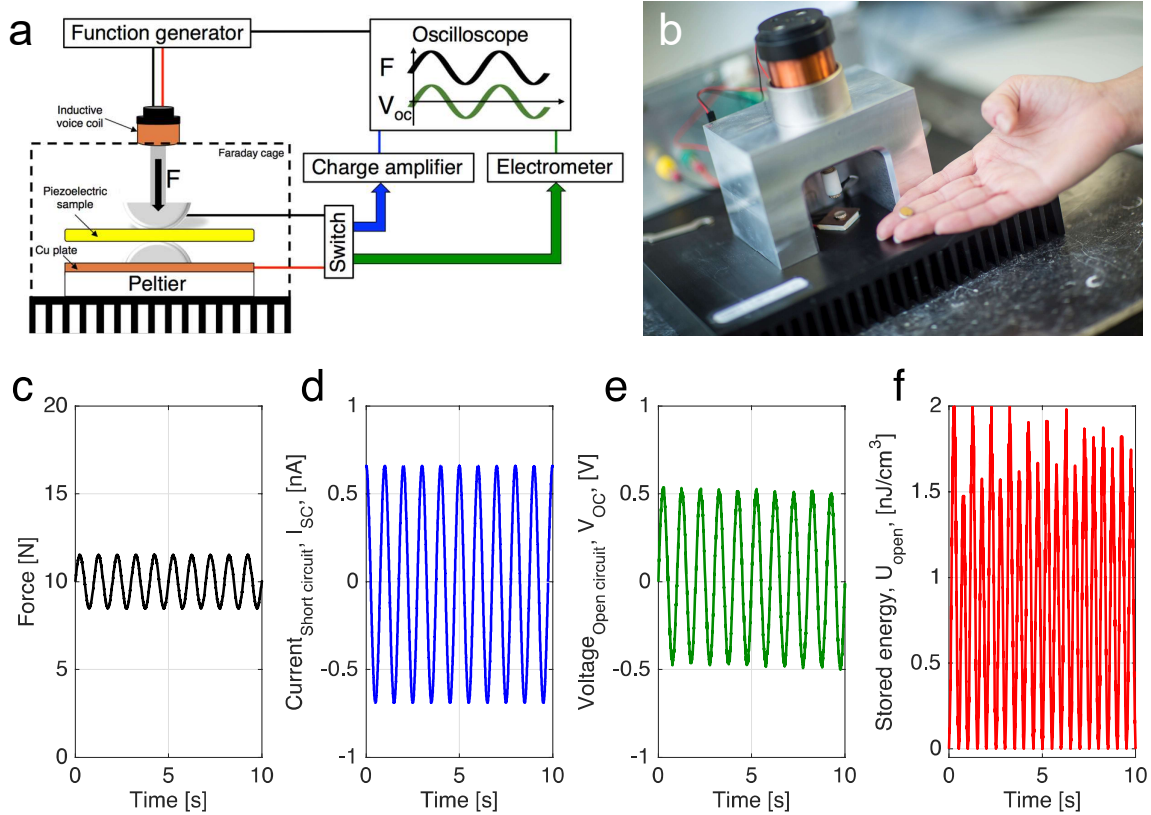

Figure 1. *Developed piezometer system. (a) Schematic representation of the measurement system. (b) Picture of the jig. (c) Example periodic input waveform of the applied force with a sinusoidal excitation of 1 Hz. (d) The short circuit current, I_{SC}, due the sinusoidal excitation shown in (c) of a PZ27 ceramic disk. (e) The corresponding open circuit voltage, V_{OC}. (f) The corresponding stored electrical energy, per unit volume, U_{open}.*

4. Experimental

The electric displacement, D, as function of electric field, E, was measured in a RT6000HVA-2 High Voltage Tester (Radiant Technologies, Albuquerque, NM, USA). The piezoelectric charge coefficient, d_{33}, was measured with a Berlincourt type piezometer (PM300, Piezotest, London, UK). A static force of 10 N was used, under a 0.25 N peak to peak sinusoidal excitation at 110 Hz. The capacitance, C, and dielectric loss, $tan\ \delta_e$, at 1 kHz and 1 V were measured with an Agilent 4263B LCR meter (Santa Clara, CA, USA) and, preceding each frequency sweep of the impedance analyzer. The dielectric constant, ε_{33}, measured under zero stress, was derived from the capacitance. The stored electrical energy, U_{open}, was measured on a variety of piezoelectric samples in the developed piezometer system. The samples were driven at 23 °C with a sinusoidal excitation amplitude of 3 N peak to peak, at 10 Hz, and clamped at 10 N, unless mentioned otherwise.

First the 'as-received' (piezo-)electric properties of four sizes (thickness of 0.5 or 1.0 mm and diameter of 10 or 20 mm) of commercially produced soft PZT (PZ27 – Ferroperm) piezoelectric ceramic disks were fully characterized, *e.g.*, for remanent polarization, coercive field, and piezoelectric coefficients. 1-3 fiber composites, denoted by 'A', were obtained from Smart Materials GmbH (Dresden, Germany) with a thickness of 1.54 mm, a PZT (SP53) filler content of 48 vol.% in an epoxy matrix, and a fiber diameter of 800 μm. A 30 μm thick film of β–phase PVDF was obtained from Images SI Inc. (PZ-04, Staten Island, NY, USA), denoted by 'B'. Three randomly distributed, 0-3, particle composites, denoted by 'C','D' and 'E', were prepared from solid state sintered ceramics embedded in a polymer matrix.[57-59] Composites 'C' and 'D' consist of 30 vol.% soft PZT-5 (Morgan Electroceramics, Ruabon, UK), in a Zn-doped ionomer (Surlyn 9320, DuPont, Barueri, SP Brazil) and an epoxy (302-3M Epotek, Epoxy Technology Inc., Billerica (MA), USA) matrix, respectively. Composite 'E' consists of 50 vol.% of Li, $K_{0.485}Na_{0.485}Li_{0.03}NbO_3$ (KNLN) embedded in a PDMS matrix. Two dielectrophoretially aligned, quasi 1-3, particle composites, denoted by 'F' and 'G', were prepared from solid state sintered ceramics, PZT-5A and KNLN, embedded in the same epoxy matrix.[60, 61]

5.   Scaling of the Stored Electrical Energy with Sample Dimensions

To validate the scaling of the stored energy per unit volume, U_{open}, with sample dimension, applied force and piezoelectric constants, *c.f.* eqn. (20), we used the intermediate polarization states of piezoceramic PZ27 as a model system. We start from a thermally depolarized PZ27 disc, by annealing for 1 h at 500 °C. The residual d_{33} then is less than 5 pC/N. Subsequently, we measured the electrical displacement as a function of applied electric field. The maximum applied voltage is ramped in small steps from 200 V to 2000 V, corresponding to a maximum applied electric field of 4 kV/mm. The measured displacement as a function of applied electric field is presented in Fig. 2a. With increasing applied voltage the inner loops gradually open until at high bias the fully saturated hysteresis loop is obtained. The remanent polarization, *i.e.* the displacement at zero bias, is derived as 34.5 $\mu C/cm^2$ and the coercive field obtained is 1.7 kV/mm, both in perfect agreement with reported literature values. We note that retention measurements have shown that the intermediate polarization states are stable over time, up to the Curie temperature.[62] The remarkable stability originates from the coexistence of effectively independent domains, with slightly different values of the coercive field.
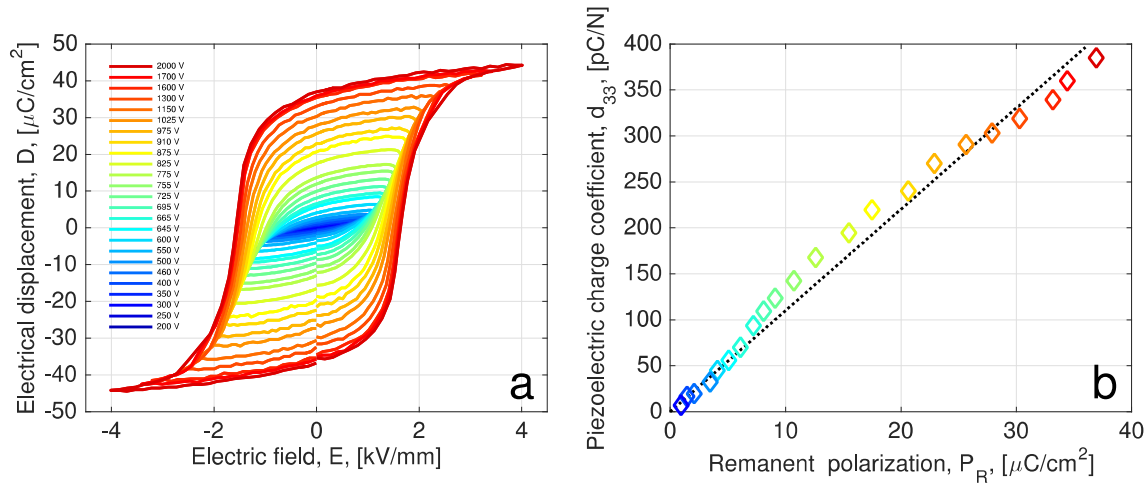

Figure 2. *Piezoelectric charge coefficient of intermediate polarization states. (a) Hysteresis loops of a representative thermally de-poled PZ27 ceramic disk as a function of electric field, E. The applied maximum field is increased in small steps, indicated by the bias given in the legend. (b) Corresponding piezoelectric charge coefficient, d_{33}, as a function of the remanent polarization, P_R. The colors of the experimental points correspond to the applied poling voltages of Fig. 2a.*

For each set value of the polarization state, we measured the piezoelectric charge coefficient. The values of d_{33} are presented as a function of the remanent polarization in Fig. 2b. A linear dependence is obtained, with a slope of 1.0 10^{-9} m²/ N. The order of magnitude is dominated by polarization induced electrostriction, as discussed in more detail in the ESI Section 6.
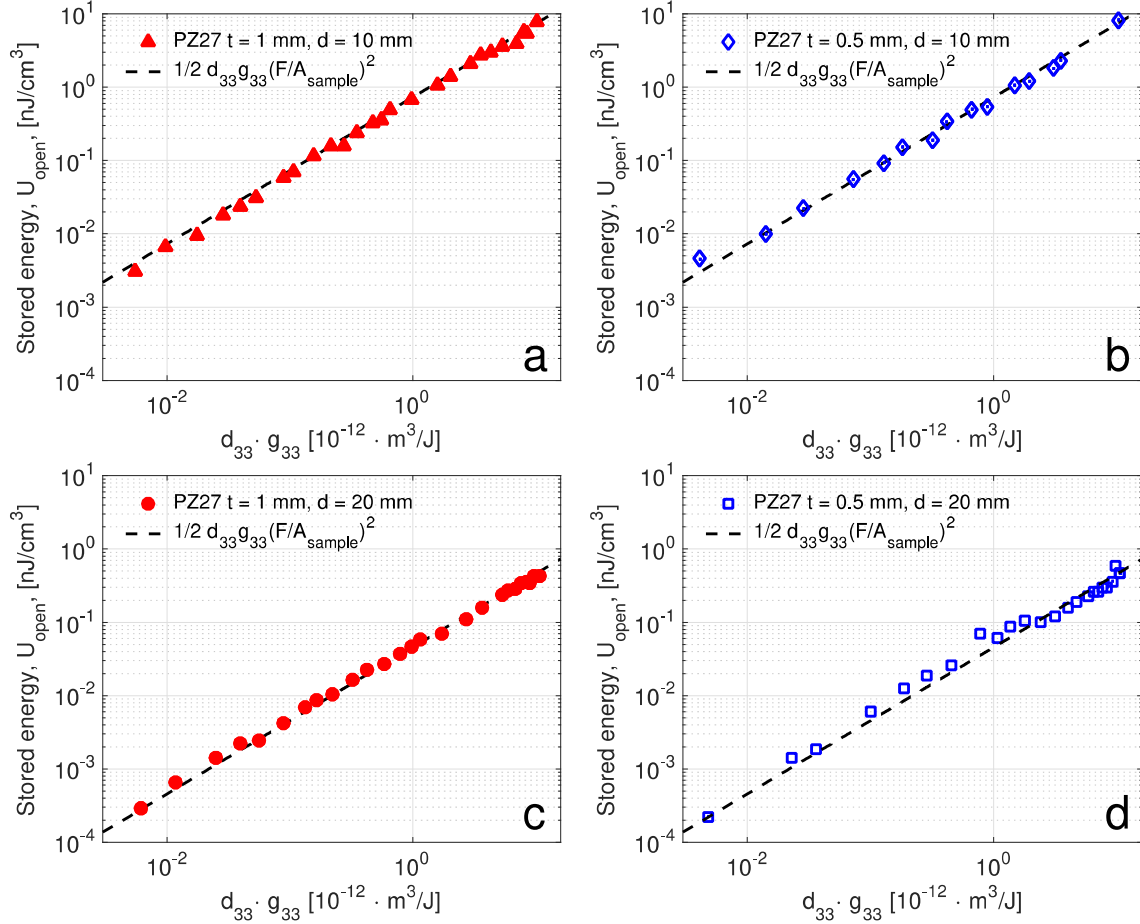

Figure 3. *Stored electrical energy as relates to figure of merit. (a) Stored electrical energy generated, U_{open}, as a function of the intermediate figure of merit, $d_{33}g_{33}$, of a PZ27 ceramic disk, of 1 mm thickness and 10 mm diameter, due to a sinusoidal excitation, F, of 3 N peak to peak. The dashed line is the verification of the measured U_{open}, calculated using eqn. (16), or ½$d_{33}g_{33}(F/A)^2$. (b) The corresponding U_{open} of a PZ27 disk of 0.5 mm thickness and 10 mm diameter. (c) The corresponding U_{open} of a PZ27 disk of 1 mm thickness and 20 mm diameter. (d) The corresponding U_{open} of a PZ27 disk of 0.5 mm thickness and 20 mm diameter.*

The stored electrical energy, per unit volume, is presented on a double logarithmic scale as a function of $d_{33}g_{33}$ in Fig. 3a-d. The piezoelectric voltage coefficient, g_{33}, was calculated by using the independently measured dielectric constant. Each figure corresponds to a different capacitor, and each point represents a different intermediate polarization state. Comparison of Fig. 3a with Fig. 3b, and of Fig. 3c with Fig. 3d, shows that the stored energy is independent of the thickness of the capacitors. Comparison of Fig. 3a with Fig. 3c, and of Fig. 3b with Fig. 3d, shows that the stored energy scales inversely with the electrode area. Furthermore, the dashed lines in Fig. 3a,d are calculated using $U_{open} = \frac{1}{2}dg\left(F/A_{sample}\right)^2$, c.f. eqn. (20). Without any adjustable fit constants, for all capacitors and intermediate polarization states a perfect agreement is obtained.

6.   Experimental Validation of the Figure of Merit

For PZ27 the stored electrical energy scales with dg. To verify this agreement is generic for any piezoelectric capacitor, we repeated the measurements using a wide variety of piezoelectric materials. We used β-phase PVDF; random 0-3 composites consisting of KNLN in PDMS and PZT in a Zn ionomer or epoxy matrix; a 1-3 composite comprising PZT in epoxy; and quasi 1-3 composites comprising dielectrophoretically aligned PZT or KNLN in an epoxy matrix. All capacitors, but the 30 μm thick PVDF film, had a similar thickness of 1 mm, and an electrode diameter of 10 mm. The open circuit output voltage was measured under sinusoidal force of 3 N peak to peak. The stored electrical energy, per unit volume, is presented as a function of the independently extracted values of $d_{33}g_{33}$ in Fig. 4a. The dashed line is calculated using eqn. (20). A perfect agreement, with an accuracy above 90%, is obtained.

As a final confirmation we deliberately varied the applied dynamic force between 1.0 N to 10 N peak to peak. The stored electrical energy is presented as a function of applied force on a double logarithmic scale in Fig. 4b. For each material investigated the stored electrical energy increases with the applied force squared.

We note that the clamped condition is a perfect model system to compare the performance of piezoelectric materials, but it is the least efficient for transferring an applied load into elastic strain energy. For instance, as shown in ESI Section 3, the calculated elastic strain energy of a clamped PZT plate, of dimensions 1 x 1 x 0.1 cm, at an applied force of 10 N is only 5.95 nJ.

Assuming the electromechanical coupling is unaffected by the change in boundary conditions from a clamped plate to a cantilever unimorph, the stored electrical energy is expected to increase about six orders of magnitude to about 0.58 mJ/cm^3. When a piezoelectric harvester is actuated at 10 Hz, under the same measurement conditions as used in this work, the stored electrical power would then be 5.8 mW/cm^3. This order of magnitude perfectly fits the estimations for the generated power per unit volume.[12, 13]

In summary, we experimentally validated that the stored electrical energy, per unit volume, under a single sinusoidal excitation, is independent of the thickness of the capacitor. The energy scales with the inverse of the electrode area, which confirms that the stored energy does not depend on the area of the caliber, as long as it is smaller than the metallized electrode area. The stored energy is proportional to the applied force squared and to the product of the piezoelectric constants $d_{33}g_{33}$ which was varied over three orders of magnitude, from 10^{-2} pm^3/J to 10 pm^3/J. In Fig. 4c we combined all the measured data in a masterplot of piezoelectric materials. The collapsed data implies that the expression derived for the stored energy, $U_{open} = \frac{1}{2}d_{33}g_{33} (F_{peak\ to\ peak}/A_{sample})^2$ holds for any piezoelectric material, irrespective of chemical composition or microstructure. We show in ESI Section 7 that this eqn. (16) automatically leads to the expression for the output power of a basic vibration-based generator in resonance, as derived in the seminal paper of Roundy.[53]

We note that the figure of merit does not depend on the compliance. This is an important conclusion as it widens the search region for potentially attractive energy harvesting materials enormously. Inorganic piezoelectric materials are brittle and prone to break. Mechanically flexible materials such as piezoelectric polymers and inorganic/organic composites will easily survive a wide range of loading conditions without fracturing. For the envisaged applications of flexible energy harvesters we refer to references [10, 18, 19, 43, 44]. Their application in energy harvesters, however, is as yet not considered as they exhibit a low value of k^2, due to a low value of the Young's modulus. However, from Fig. 4c we can deduce that flexible, piezoelectric materials, can exhibit a high value of dg. The highest measured stored energies comprise both a low Young's modulus particle composite and a 1-3 fiber composite.
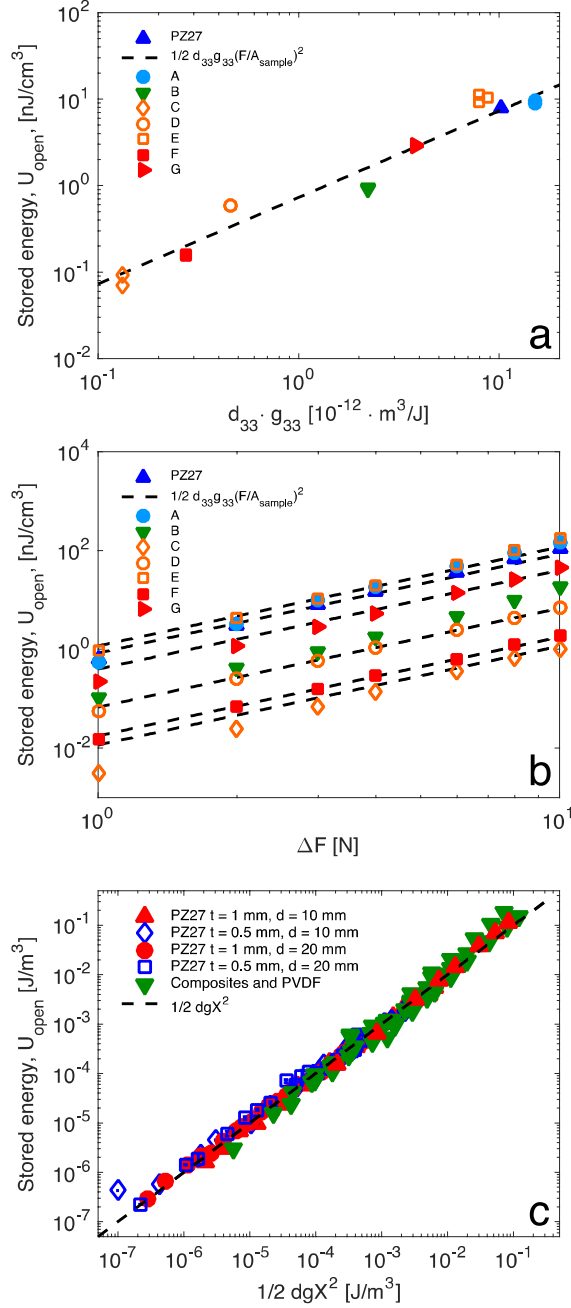
Figure 4. *Figure of merit as relates to the stored electrical energy of a variety of piezoelectric material classes. (a) Stored electrical energy, per unit volume, as a function of the figure of merit ($d_{33}g_{33}$). The dashed line is the verification of U_{open}, per eqn. (16), or $\frac{1}{2}d_{33}g_{33}(F/A)^2$, for a given sinusoidal force, ΔF, of 3 N peak to peak and sample area, A, of 78.5 mm^2, which corresponds to a diameter of 10 mm. (b) Stored electrical energy, per unit volume, as a function of the peak to peak value of the applied sinusoidal force, ΔF. The dashed lines represent the calculation of $\frac{1}{2}d_{33}g_{33}(F/A_{sample})^2$ for each corresponding figure of merit, $d_{33}g_{33}$, and sample area, A. (c) The reconstructed masterplot of all piezoelectric materials considered.*

7. Harvested Output Energy

To support the analysis above, we measured not only the stored electrical energy, but also the harvested output energy. There are many methods to transfer stored electrical energy to the outside world, such as rectifying diode rings or inductive coils. Here we did not optimize the electrical-electrical conversion, but used a resistive load. The piezoelectric capacitor was excited with a single sinusoidal excitation as described above. The output power was measured and plotted as a function of the resistive load. A parabola was obtained, with a maximum power point occurring when the impedance of the resistive load was equal to the impedance of the piezoelectric capacitor. The ratio of output power over the stored electrical power in open circuit conditions, $U_{out,max} / U_{open}$, is presented in Fig. 5 as a function of the electromechanical coupling coefficient, k^2. The ratio $U_{out,max} / U_{open}$ was taken as $(V_{max\ power\ point} / V_{open\ circuit})^2$ and values of k^2 were calculated from eqn. (6). The power ratio is about 0.12 at low values of k^2 and increases to about 0.45 at values of k^2 approaching unity. The solid line is calculated as $1/(4-2k^2)$, as derived from the analytical derivation of the maximum output energy in section 2.4, *c.f.* eqn. (16). The deviation is a factor of two. The reason is that the calculated maximum output energy assumes 100% efficiency for the conversion of output energy into the electrical energy of the circuit. For the resistive load used here, we calculate that this electrical-electrical conversion efficiency is about 50%, see ESI Section 9. Taking this factor into account, the dashed line is calculated, and a good agreement is obtained, validating that the output energy of an energy harvester, per unit volume, $U_{out,max}$, is given as $1/(4-2k^2)*\frac{1}{2}dgX^2$, as analytically derived in eqn. (16).
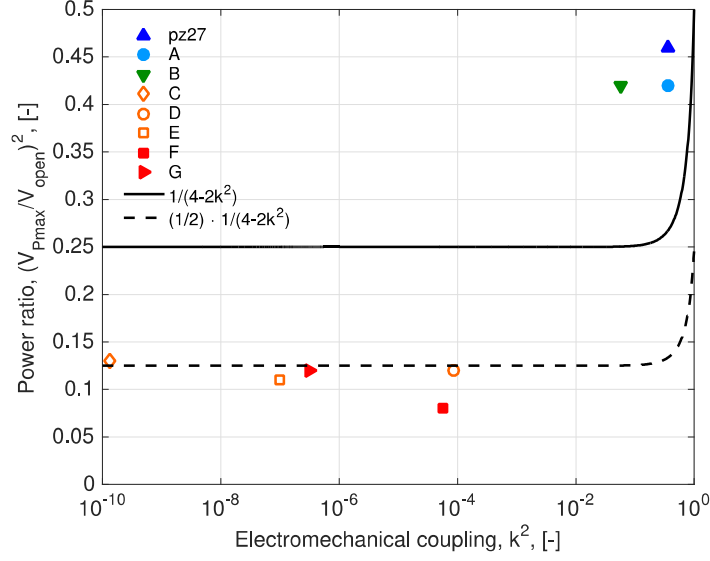
Figure 5. *Maximum output energy over stored electrical energy in open circuit conditions as a function of electromechanical coupling coefficient, k^2. The solid line is calculated as $1/(4-2k^2)$, while the dashed line is calculated as $(1/2)\ 1/(4-2k^2)$.*

8.   Conclusions

We have analytically derived that for an energy harvester, comprising a piezoelectric capacitor with mechanical load, the maximum output energy per unit volume, under a single sinusoidal excitation, is given by $1/(4-2k^2)*\ \frac{1}{2}dgX^2$. A sensitive piezometer system was developed that, with high accuracy, could measure the output energy under sinusoidal excitation. The output energy was measured for intermediate polarization states of a PZT piezoceramic, and for a wide variety of ferroelectric materials. The experimentally measured output energy could perfectly be described, over more than five orders of magnitude. The prefactor $1/(4-2k^2)$ varies only between ¼ and ½ meaning that the figure of merit of a piezoelectric energy harvester is not k^2, as until now generally accepted for vibrational energy harvesters, but *dg*.

Acknowledgements

Conflicts of Interest

There are no conflicts to declare.

References

1.   M. Umeda, K. Nakamura and S. Ueha, *Japanese Journal of Applied Physics*, 1996, **35**, 3267-3273.

2.   N. S. Shenck and J. A. Paradiso, *IEEE micro*, 2001, **21**, 30-42.

3.   G. Park, T. Rosing, M. D. Todd, C. R. Farrar and W. Hodgkiss, *Journal of Infrastructure Systems*, 2008, **14**, 64-79.

4.   S. Priya and D. J. Inman, *Energy harvesting technologies*, Springer, New York, NY, USA, 2009.

5.   M. Ferrari, V. Ferrari, M. Guizzetti and D. Marioli, *Smart Materials and Structures*, 2009, **18**, 085023.

6.   M. Renaud, P. Fiorini, R. van Schaijk and C. van Hoof, *Smart Materials and Structures*, 2012, **21**, 049501.

7.   C. Dagdeviren, B. D. Yang, Y. Su, P. L. Tran, P. Joe, E. Anderson, J. Xia, V. Doraiswamy, B. Dehdashti, X. Feng, B. Lu, R. Poston, Z. Khalpey, R. Ghaffari, Y. Huang, M. J. Slepian and J. A. Rogers, *Proc Natl Acad Sci U S A*, 2014, **111**, 1927-1932.

8.   G.-T. Hwang, V. Annapureddy, J. H. Han, D. J. Joe, C. Baek, D. Y. Park, D. H. Kim, J. H. Park, C. K. Jeong, K.-I. Park, J.-J. Choi, D. K. Kim, J. Ryu and K. J. Lee, *Advanced Energy Materials*, 2016, **6**, 1600237.

9.   S. P. Beeby, M. J. Tudor and N. M. White, *Measurement Science and Technology*, 2006, **17**, R175-R195.

10.   K. A. Cook-Chennault, N. Thambi, M. A. Bitetto and E. B. Hameyie, *Bulletin of Science, Technology & Society*, 2006, **28**, 496-509.

11.   P. D. Mitcheson, E. M. Yeatman, G. K. Rao, A. S. Holmes and T. C. Green, *Proceedings of the IEEE*, 2008, **96**, 1457-1486.

12.   S. Roundy, P. K. Wright and R. J., *Compute Communications*, 2003, **26**, 1131-1144.

13.   E. Lefeuvre, A. Badel, A. Benayad, L. Lebrun, C. Richard and D. Guyomar, *Journal de Physique IV (Proceedings)*, 2005, **128**, 177-186.

14.   H. Li, C. Tian and Z. D. Deng, *Applied Physics Reviews*, 2014, **1**, 041301.

15. H. A. Sodano, D. J. Inman and G. Park, *The Shock and Vibration Digest*, 2004, **36**, 197-205.

16. S. Priya, *Journal of Electroceramics*, 2007, **19**, 167-184.

17. T. Rödig, A. Schönecker and G. Gerlach, *Journal of the American Ceramic Society*, 2010, **93**, 901-912.

18. H. S. Kim, J.-H. Kim and J. Kim, *International Journal of Precision Engineering and Manufacturing*, 2011, **12**, 1129-1141.

19. C. R. Bowen, H. A. Kim, P. M. Weaver and S. Dunn, *Energy & Environmental Science*, 2014, **7**, 25-44.

20. H. W. Kim, A. Batra, S. Priya, K. Uchino, D. Markley, R. E. Newnham and H. F. Hofmann, *Japanese Journal of Applied Physics*, 2004, **43**, 6178-6183.

21. P. J. Cornwell, J. Goethal, J. Kowko and M. Damianakis, *Journal of Intelligent Material Systems and Structures*, 2005, **16**, 825-834.

22. J. H. Cho, R. F. Richards, D. F. Bahr, C. D. Richards and M. J. Anderson, *Applied Physics Letters*, 2006, **89**, 104107.

23. J. Ajitsaria, S. Y. Choe, D. Shen and D. J. Kim, *Smart Materials and Structures*, 2007, **16**, 447-454.

24. A. Erturk and D. J. Inman, *Smart Materials and Structures*, 2009, **18**, 025009.

25. C. Mo, J. Davidson and W. W. Clark, *Smart Materials and Structures*, 2014, **23**, 045005.

26. S. Roundy and Y. Zhang, 2005.

27. E. S. Leland and P. K. Wright, *Smart Materials and Structures*, 2006, **15**, 1413-1420.

28. H. Xue, Y. Hu and Q.-M. Wang, *IEEE Transactions on Ultrasonics, Ferroelectrics and Frequency Control*, 2008, **55**.

29. K. Uchino, *Sci Technol Adv Mater*, 2015, **16**, 046001.

30. J. Rödel, K. G. Webber, R. Dittmer, W. Jo, M. Kimura and D. Damjanovic, *Journal of the European Ceramic Society*, 2015, **35**, 1659-1681.

31. H. A. Sodano, D. J. Inman and G. Park, *Journal of Intelligent Material Systems and Structures*, 2005, **16**, 67-75.

32. G. K. Ottman, H. F. Hofmann, A. C. Bhatt and G. A. Lesieutre, *IEEE Transactions on Power Electronics*, 2002, **17**, 669-676.

33. D. Guyomar, G. Sebald, S. Pruvost, M. Lallart, A. Khodayari and C. Richard, *Journal of Intelligent Material Systems and Structures*, 2008, **20**, 609-624.

34. C. D. Richards, M. J. Anderson, D. F. Bahr and R. F. Richards, *Journal of Micromechanics and Microengineering*, 2004, **14**, 717-721.

35. C. Rendl, P. Greindl, M. Haller, M. Zirkl, B. Stadlober and P. Hartmann, 2012.

36. Y. Mao, P. Zhao, G. McConohy, H. Yang, Y. Tong and X. Wang, *Advanced Energy Materials*, 2014, **4**, 1301624.

37. W.-S. Jung, M.-J. Lee, M.-G. Kang, H. G. Moon, S.-J. Yoon, S.-H. Baek and C.-Y. Kang, *Nano Energy*, 2015, **13**, 174-181.

38. R. Patel, Y. Tanaka, S. McWilliam, H. Mutsuda and A. A. Popov, *Journal of Sound and Vibration*, 2016, **368**, 87-102.

39. S. Bauer, R. Gerhard-Multhaupt and G. M. Sessler, *Physics Today*, 2004, **57**, 37-43.

40. S. Bauer and F. Bauer, in *Piezoelectricity*, Springer, Berlin, Germany, 2008, pp. 157-177.

41. W. Li, D. Torres, T. Wang, C. Wang and N. Sepúlveda, *Nano Energy*, 2016, **30**, 649-657.

42. K. I. Park, M. Lee, Y. Liu, S. Moon, G. T. Hwang, G. Zhu, J. E. Kim, S. O. Kim, D. K. Kim, Z. L. Wang and K. J. Lee, *Advanced Materials*, 2012, **24**, 2999-3004, 2937.

43. J. Briscoe and S. Dunn, *Nano Energy*, 2015, **14**, 15-29.

44. F. R. Fan, W. Tang and Z. L. Wang, *Advanced Materials*, 2016, **28**, 4283-4305.

45. R. A. Islam and S. Priya, *Journal of the American Ceramic Society*, 2006, **89**, 3147-3156.

46. H. Kim, S. Priya, H. Stephanou and K. Uchino, *IEEE Transactions on Ultrasonics, Ferroelectrics and Frequency Control*, 2007, **54**, 1851-1859.

47. J. Liang and W.-H. Liao, *Smart Materials and Structures*, 2011, **20**, 015005.

48. K. Wasa, T. Matsushima, H. Adachi, I. Kanno and H. Kotera, *Journal of Microelectromechanical Systems*, 2012, **21**, 451-457.

49. N. Chidambaram, A. Mazzalai and P. Muralt, *IEEE Trans Ultrason Ferroelectr Freq Control*, 2012, **59**, 1624-1631.

50. C.-H. Choi, I.-T. Seo, D. Song, M.-S. Jang, B.-Y. Kim, S. Nahm, T.-H. Sung and H.-C. Song, *Journal of the European Ceramic Society*, 2013, **33**, 1343-1347.

51. Y. Zhang, M. Xie, J. Roscow, Y. Bao, K. Zhou, D. Zhang and C. R. Bowen, *J Mater Chem A*, 2017, **5**, 6569-6580.

52. Q. M. Wang, X. H. Du, B. Xu and L. E. Cross, *IEEE Transactions on Ultrasonics, Ferroelectrics and Frequency Control*, 1999, **46**, 638-646.

53. S. Roundy, *Journal of Intelligent Material Systems and Structures*, 2005, **16**, 809-823.

54. K. Uchino, *Ferroelectric devices & Piezoelectric actuators*, DEStech Publications Inc. , Lancaster, PA, USA, 10 edn., 2017.

55. D. Damjanovic, *Journal of Applied Physics*, 1997, **82**, 1788-1797.

56. O. Guillon, F. Thiebaud and D. Perreux, *International Journal of Fracture*, 2002, **117**, 235-246.

57. N. K. James, U. Lafont, S. van der Zwaag and W. A. Groen, *Smart Materials and Structures*, 2014, **23**, 055001.

58. F. Van Loock, D. B. Deutz, S. van der Zwaag and W. A. Groen, *Smart Materials and Structures*, 2016, **25**, 085039.

59. N. T. Mascarenhas, Delft University of Technology, 2015.

60. D. A. van den Ende, B. F. Bory, W. A. Groen and S. van der Zwaag, *Journal of Applied Physics*, 2010, **107**, 024107.

61. D. B. Deutz, N. T. Mascarenhas, S. van der Zwaag and W. A. Groen, *Journal of the American Ceramic Society*, 2017, **100**, 1108-1117.

62. D. Zhao, I. Katsouras, K. Asadi, W. A. Groen, P. W. M. Blom and D. M. de Leeuw, *Applied Physics Letters*, 2016, **108**, 232907.